

GSI

GSI-Preprint-99-09
Februar 1999

NEW RESULTS ON THE HALO STRUCTURE OF ${}^8\text{B}$

M.H. Smedberg, T. Baumann, T. Aumann, L. Axelsson,, U. Bergmann,
M.J.G. Borge, D. Cortina-Gil, L.M. Fraile, H. Geissel, L. Grigorenko,
M. Hellström, M. Ivanov, N. Iwasa, R. Janik, B. Jonson, H. Lenske,
K. Markenroth, G. Münzenberg, T. Nilsson, A. Richter, K. Riisager,
C. Scheidenberger, G. Schrieder, W. Schwab, H. Simon, B. Sitar, P. Strmen,
K. Sümmerer, M. Winkler, M.V. Zhukov

CERN LIBRARIES, GENEVA



CM-P00066921

Gesellschaft für Schwerionenforschung mbH
Planckstraße 1 • D-64291 Darmstadt • Germany
Postfach 11 05 52 • D-64220 Darmstadt • Germany

New results on the halo structure of ${}^8\text{B}$

M.H. Smedberg^a, T. Baumann^b, T. Aumann^b, L. Axelsson^a,
U. Bergmann^c, M.J.G. Borge^d, D. Cortina-Gil^b, L.M. Fraile^d,
H. Geissel^b, L. Grigorenko^a, M. Hellström^{b,1}, M. Ivanov^e,
N. Iwasa^{b,2}, R. Janik^e, B. Jonson^a, H. Lenske^g,
K. Markenroth^a, G. Münzenberg^b, T. Nilsson^f, A. Richter^h,
K. Riisager^c, C. Scheidenberger^b, G. Schrieder^h, W. Schwab^b,
H. Simon^h, B. Sitar^e, P. Strmen^e, K. Sümmerer^b,
M. Winkler^b, M.V. Zhukov^a

^a*Fysiska Institutionen, Chalmers Tekniska Högskola, S-41296 Göteborg, Sweden*

^b*Gesellschaft für Schwerionenforschung, D-64291 Darmstadt, Germany*

^c*Institut for Fysik og Astronomi, Aarhus Universitet, DK-8000 Aarhus C, Denmark*

^d*Instituto Estructura de la Materia, CSIC, E-28006 Madrid, Spain*

^e*Comenius University, 84215 Bratislava, Slovakia*

^f*EP Division, CERN, CH-1211 Genève 23, Switzerland*

^g*Institut für Theoretische Physik, Universität Giessen, D-35392 Giessen, Germany*

^h*Institut für Kernphysik, Technische Universität, D-64289 Darmstadt, Germany*

The longitudinal momentum distribution of ${}^7\text{Be}$ fragments after fragmentation of ${}^8\text{B}$ and the one-proton removal cross section (σ_{-1p}) in a carbon target were measured at 1440 MeV/u with the fragment separator FRS used as an energy-loss spectrometer. The results show a narrow momentum distribution with a FWHM value of 91 ± 5 MeV/c and a large cross-section, $\sigma_{-1p} = 98 \pm 6$ mb. Both these results support the interpretation of a spatially extended proton orbit forming a halo in the ${}^8\text{B}$ ground state. The momentum distribution and the one-proton removal cross section are shown to be reproduced with a three-body wave function for ${}^8\text{B}$ where the target is treated as a black disc in the breakup process.

PACS: 25.60.Gc, 27.20.+n

Key words: unstable nuclei, breakup reactions, momentum distributions, one-proton removal cross section, nuclear structure

80 2712-142

1 Introduction

The first observation of a narrow width in the longitudinal momentum distribution of the ${}^7\text{Be}$ fragments from ${}^8\text{B}$ breakup reactions [1] sparked off an intense research concerning the proton dripline nucleus ${}^8\text{B}$. The ground state of ${}^8\text{B}$, with a proton separation energy of 138 keV [2], is the only known one-proton halo candidate besides the first excited state in ${}^{17}\text{F}$ [3,4]. However, the formation of an extended proton distribution is hindered by the Coulomb barrier and the $l=1$ angular momentum barrier seen by the valence proton, therefore the interpretation in terms of a proton halo in ${}^8\text{B}$ is still controversial. A second reason for particular interest in ${}^8\text{B}$ is its role in the solar neutrino problem (see Ref. [5] and references therein).

Previous measurements of the longitudinal momentum distribution of ${}^7\text{Be}$ fragments from ${}^8\text{B}$ breakup reactions show narrow widths [1,6,7] compared to the statistical model of Goldhaber [8]. The first set of data taken at GSI [1] at a beam energy of 1471 MeV/u showed the same width of 81 ± 6 MeV/c (FWHM) for all target nuclei used (C, Al, Pb). The rather narrow width was interpreted as a large spatial extension of the loosely bound proton. Similar measurements have later been performed at MSU [6], but at a lower beam energy of 41 MeV/u. Here, the FWHM value showed a dependence on the target charge, giving FWHM values of 81 ± 4 MeV/c on beryllium and 62 ± 3 MeV/c on gold targets. The authors of Ref. [6] found that the reaction mechanism significantly narrows the ${}^7\text{Be}$ momentum distribution, so it does not directly reflect the intrinsic proton momentum wave function. This is in contrast to the one-neutron halo nucleus ${}^{11}\text{Be}$, where the halo size is roughly reciprocally proportional to the observed momentum width. Such a connection is only valid in the limit of small separation energy and if the valence nucleon is a neutron in an s -wave, whereas the valence nucleon in ${}^8\text{B}$ is a proton mainly bound in a p -orbit. Calculating the $p_{3/2}$ valence proton state in a Woods-Saxon geometry, an intrinsic longitudinal momentum width around 150 MeV/c is typically found [6,9]. Although this width considerably exceeds the value found for s -wave neutron-halo states, it is still about a factor of 2 smaller than for well-bound p -states in this mass region (~ 250 – 300 MeV/c). The proton stripping process on the beryllium target reduces this width to 82 MeV/c [9], in agreement with experimental data. The longitudinal momentum distribution of ${}^7\text{Be}$ from ${}^8\text{B}$ breakup reactions on silicon has been studied at GANIL [7] at a beam energy of 38 MeV/u, giving a FWHM value of 93 ± 7 MeV/c.

In this paper we present the result of a new measurement of ${}^8\text{B}$ breakup reactions performed at GSI at 1440 MeV/u. The new experiment was con-

¹ Present Address: Fysiska Institutionen, Lunds Universitet, S-22100 Lund, Sweden

² Present Address: RIKEN, 2-1 Hirosawa, Wako, Saitama 351-01, Japan

siderably improved in two points compared to the previous one [1]. First, the new data was taken with much better statistics, and second, the ${}^7\text{Be}$ longitudinal momentum distribution was taken with three different $B\rho$ settings and therefore for the first time a good determination of the high momentum tail was obtained. We also present theoretical calculations which reproduce the experimental result well.

2 Experimental setup

The secondary ${}^8\text{B}$ beam was produced by fragmentation of a 1.5 GeV/u ${}^{12}\text{C}$ beam from the heavy-ion synchrotron SIS in a 8.0 g/cm² Be target placed at the entrance of the magnetic spectrometer FRS [10]. In order to measure the longitudinal momentum distribution of ${}^7\text{Be}$ fragments, the FRS was operated as an energy-loss spectrometer in the manner described in Ref. [15]. In the energy-loss mode, the large momentum spread caused by the ${}^8\text{B}$ production process does not contribute to the measured momentum width of the ${}^7\text{Be}$ fragments. The magnetic fields of the first two dipole stages of the FRS were set to select the beam of ${}^8\text{B}$. Due to the magnetic rigidity analysis of the first spectrometer stage and the fact that the neighboring boron isotopes are unbound, ${}^8\text{B}$ could be unambiguously identified by the energy deposition measured with a scintillation detector located in front of the breakup target. The ${}^8\text{B}$ beam, with an energy of 1440 MeV/u, impinged on the 4.41 g/cm² carbon breakup target that was placed at the dispersive mid-plane of the FRS. The spectrometer stage behind the breakup target was set to a magnetic rigidity corresponding to a ${}^7\text{Be}$ ejectile produced in a one-proton removal reaction. Fragments arriving at the final focus were identified by measuring the time-of-flight in the second spectrometer stage, by determining the magnetic rigidity from the position measurement at the final focal plane, and by a coincident energy-deposition measurement in an ionisation chamber.

The ${}^7\text{Be}$ longitudinal momentum distribution is directly deduced from the position measurements at the final focal plane using the experimentally determined dispersion. Ion-optical aberrations and atomic energy straggling in the relatively thick breakup target limit the resolution that can be achieved in this measurement. These contributions, which broaden the measured width, were quantified by measuring the position distribution of ${}^8\text{B}$ that penetrated the breakup target without nuclear reactions. The breakup of the projectile nuclei is statistically distributed along their path inside the target, which causes an additional energy straggling due to the difference in energy loss between ${}^8\text{B}$ and ${}^7\text{Be}$. This contribution was calculated using the ion-optical ray tracing code MOCADI [16]. In total, the experimental resolution was determined to be 20 MeV/c (FWHM) which results in a correction for the measured width of 2%.

3 Experimental results and discussion

In Figure 1 we present the longitudinal momentum distribution of ${}^7\text{Be}$, transformed into the ${}^8\text{B}$ projectile frame. In order to cover a large range of momenta, the distribution was recorded at three different $B\rho$ -settings. Starting at a central setting, the magnetic rigidity $B\rho$ of the stages behind the breakup target was increased by 1% for each further setting to measure the distribution at large positive longitudinal momenta (see Figure 1). The experimental distribution displayed in Figure 1 (filled circles) has a FWHM value of 93 ± 5 MeV/c. After correction for the experimental resolution, this gives a width of 91 ± 5 MeV/c. The histogram in the figure shows the data from Ref. [1]. This distribution, from which a FWHM of 81 ± 6 MeV/c was obtained, agrees well with the new data in the central region. The new measurement covers, however, also the high-momentum tail which allows a more complete analysis of the line shape. The experimental one-proton removal cross-section obtained in this measurement is 98 ± 6 mb (see also [11]), which agrees nicely with the earlier result of 94 ± 4 mb [1]. The one-proton removal cross section is enhanced by almost a factor 2 as compared to the case of a tightly bound proton. This is an additional signature for an extended valence-proton wave function [12].

In the previous papers [1,6,7], where the ${}^8\text{B}$ breakup to the ${}^7\text{Be}$ channel was studied, various theoretical models were used for comparison with experimental data. For such a comparison, one needs first of all a wave function of ${}^8\text{B}$. In Ref. [1], ${}^8\text{B}$ was described in a mean field and RPA approach. Recently this approach has been improved considerably [13,14] leading to a rms-radius of 2.58 fm for ${}^8\text{B}$ and an rms-distance of 4.73 fm for the ${}^7\text{Be}$ -proton system thus reducing considerably the values quoted in Ref. [1]. In Ref. [6] a two-body potential model [9] was used to construct the ${}^7\text{Be}+p$ relative motion wave function. It used a Woods-Saxon well for the ${}^7\text{Be}$ - p potential and fitted parameters to get a correct binding energy for the $p_{3/2}$ valence proton. This yielded an rms ${}^7\text{Be}$ - p distance of 4.94 fm. In Ref. [7], a self consistent calculation of single particle wave functions was performed using shell model occupation probabilities and a constraint on the total binding energy. This model gave an rms radius for ${}^8\text{B}$ of 2.55–2.6 fm, and an rms ${}^7\text{Be}$ - p distance of 4.22–4.5 fm.

It was demonstrated in Refs. [9,17,18] that the reaction mechanism is very important and has to be included if one wants to compare predictions of theoretical models for ${}^7\text{Be}$ momentum distributions with experimental data from the ${}^8\text{B}$ breakup reactions. Note that the reaction mechanism is important also for calculations of momentum distributions of ${}^{16,18}\text{C}$ isotopes from breakup of ${}^{17,19}\text{C}$ [19,13]. However, the reaction mechanism has less importance when the ${}^{10}\text{Be}$ momentum distributions from the one-neutron halo nucleus ${}^{11}\text{Be}$ are

studied.

To describe the data in this paper, we will use the ${}^8\text{B}$ wave function calculated in an extended three-body model ($\alpha+{}^3\text{He}+p$) [20]. In this model, the ${}^8\text{B}$ nucleus is treated in the framework of three-body models with explicit inclusion of the binary ${}^7\text{Be}+p$ channel. Effects of strong deformation and dynamical polarization of the ${}^7\text{Be}$ core as well as the core excitations are treated simultaneously. The model describes the bulk properties of ${}^8\text{B}$ well and leads to an rms matter radius of 2.58–2.60 fm. An important finding is that, due to the presence of the third particle, the average distance between the α -particle and ${}^3\text{He}$ in the ${}^8\text{B}$ wave function is smaller than the one in the free ${}^7\text{Be}$ nucleus. This leads to an rms distance between ${}^7\text{Be}$ and the proton of 4.6 fm. The ${}^7\text{Be}-p$ relative motion wave functions, $F_{j_x j_y}(Y)$ with angular momentum j_y are obtained by projecting the ${}^8\text{B}$ ($J^\pi=2^+$ ground state) wave function onto the ${}^7\text{Be}$ wave functions with angular momentum j_x

$$F_{j_x j_y}(Y) = \langle \Psi_{JM}^{8\text{B}}(\mathbf{X}, \mathbf{Y}) | [\Psi_{j_x}^{7\text{Be}}(\mathbf{X}), [Y_{j_y}(\hat{n}_y), \chi_{S_3}]_{j_y}]_{JM} \rangle \quad (1)$$

where the variables X and Y are defined in the inset in Figure 2. The spectroscopic factors $S_{j_x j_y}$ are obtained by integration of $F_{j_x j_y}^2(Y)$. The dominating spectroscopic factors are $S_{3/2,3/2}=0.685$, $S_{3/2,1/2}=0.101$, and $S_{1/2,3/2}=0.083$. The first two correspond to a proton in $p_{3/2}$ and $p_{1/2}$ orbitals relative to the ${}^7\text{Be}$ ground state ($J^\pi=3/2^-$), and the third one to a proton in a $p_{3/2}$ orbital relative to the first excited state of ${}^7\text{Be}$ ($J^\pi=1/2^-$). Figure 2 displays the relative motion wave functions $Y \cdot F_{j_x j_y}(Y)$ for the three dominating channels.

At relativistic energies and on light targets the observed core fragment momentum distributions in light neutron rich nuclei have often been interpreted as the ground state momentum distributions inside the nuclei. This identification, where the reaction mechanism is assumed to be very simple and not to add modifying terms, is referred to as the transparent limit of the Serber model [21] and just corresponds to the momentum distributions calculated from the Fourier transform of the spatial wave function. The result of such a calculation for the ${}^8\text{B}$ nucleus, with the relative motion wave functions $F_{j_x j_y}(Y)$ (see equation (1)), gives a ${}^7\text{Be}$ longitudinal momentum width of 149 MeV/c for the three dominating channels. The contributions from each channel are displayed in Table 1. This value is close to other calculations [9,17], but still larger than the experimental one. An improvement of this approximation can easily be made by taking absorption into account [9,17,19,13]. In this case, the proton should be absorbed by the target nucleus and the ${}^7\text{Be}$ fragment should have an impact parameter sufficiently large to avoid a collision with the target nucleus. In this opaque limit of the Serber model, where the target is considered as a black disc, one easily derives the longitudinal momentum distribution [19] of the ${}^7\text{Be}$ fragment originating from an $l=1$ relative motion wave function $F_{j_x j_y}(Y)$,

$$\frac{d\sigma_{-p}}{dk_z} = \frac{1}{2} \int_0^{R_t+R_p} b db \int_{R_c+R_t-b}^{\infty} r_{\perp} dr_{\perp} \int_{-\infty}^{\infty} dz \int_{-\infty}^{\infty} dz' f(r_{\perp}, b) \exp(ik_z(z-z')).$$

$$F_{j_x j_y}(\sqrt{r_{\perp}^2 + z^2}) F_{j_x j_y}(\sqrt{r_{\perp}^2 + z'^2}) \frac{r_{\perp}^2 + zz'}{\sqrt{r_{\perp}^2 + z^2} \sqrt{r_{\perp}^2 + z'^2}}, \quad (2)$$

where

$$f(r_{\perp}, b) = \begin{cases} 1 - \frac{1}{\pi} \arccos\left(\frac{r_{\perp}^2 + b^2 - (R_c + R_t)^2}{2r_{\perp}b}\right) & r_{\perp} < R_c + R_t + b \\ 1 & r_{\perp} > R_c + R_t + b. \end{cases} \quad (3)$$

Here, R_c and R_t are the rms radii of the core and the target nuclei, while R_p is the proton radius. In this expression we have omitted the contribution from diffraction and Coulomb dissociation. The latter contribution should be negligible for light targets such as carbon while the former gives a momentum distribution close to that obtained in nuclear stripping [17,18]. Finally, the proton stripping cross section, σ_{-p} , is obtained by integrating equation (2) over the longitudinal momentum.

The longitudinal momentum distribution of the ${}^7\text{Be}$ fragments (from the proton stripping reaction) corresponding to the sum of the three dominating channels is shown in Figure 3 as a solid curve. This curve, folded with the experimental resolution, has been calculated according to equation (2) in absolute scale, with the parameters $R_c=2.4$ fm, $R_t=2.47$ fm, and $R_p=0.8$ fm. The corresponding cross-sections and momentum widths for the individual channels are displayed in Table 1. To investigate the line shape of our calculation we scaled our calculated solid curve in Figure 3 with a factor 1.30. The resulting dotted curve shown in Figure 3 agrees well with the data in the narrow central region as well as in the high momentum tail. The calculated proton-stripping cross-section obtained from equation (2) is in good agreement with the corresponding number in Ref. [9]. However, this number can not be directly compared to the experimental proton-removal cross-section of 98 ± 6 mb, since the ${}^7\text{Be}$ fragments can also appear from diffraction dissociation of ${}^8\text{B}$. The diffraction dissociation cross-section is smaller than the proton-stripping cross-section for beam energies around 1 GeV/u, and it accounts for about 20%–25% of the proton-stripping cross-section (see Ref. [18]). If we assume this ratio of the cross section, the total proton-removal cross-sections in our calculation can be estimated at 92–96 mb, which agrees with the result obtained in this work.

4 Summary

In this paper we have presented new experimental results on the longitudinal momentum distribution of ${}^7\text{Be}$ fragments after breakup of 1440 MeV/u ${}^8\text{B}$ in a carbon target. Improved statistics and an extended momentum coverage, as compared to our earlier measurement [1], allow a more sensitive test of the halo structure of the ${}^8\text{B}$ ground state.

The new data are compared with theoretical calculations where we have used ${}^7\text{Be}+p$ relative motion wave functions, $F_{j_x j_y}$, from the extended three-body model [20], which reproduces the ${}^8\text{B}$ bulk properties well. With these wave functions and a “black-disc” model for the proton-stripping reaction, we were able to reproduce the shape of the momentum distribution over the entire momentum range covered by this experiment.

The results show that the observed rather narrow width of 91 ± 5 MeV/c for the ${}^7\text{Be}$ fragments in the proton removal channel of the ${}^8\text{B}$ high-energy breakup is a result of a long tail of the valence proton wave function and the shadowing effect in the reaction. This fact, together with the well reproduced proton-removal cross-section in the framework of the same model, supports the picture of ${}^8\text{B}$ as a clustered system with a loosely bound p -wave proton extending beyond the ${}^7\text{Be}$ core.

This work was supported by the German Federal Minister for Education and Research (BMBF) under Contracts 06 DA 820, 06 OF 474, and 06 MZ 476 and by GSI via Hochschulzusammenarbeitsvereinbarungen under Contracts DARIK, OF ELK, and MZ KRK. It was partly supported by the Polish Committee of Scientific Research under Contract PB2/P03B/113/09, EC under Contract ERBCHGE-CT92-0003, CICYT under Contract AEN96-1679 (MJGB, LMF), and by Deutsche Forschungsgemeinschaft (DFG) under Contract 436 RUS 130/127/1 and Le-439/1. One of us (B.J.) acknowledges the support through an Alexander von Humboldt Research Award.

References

- [1] W. Schwab, H. Geissel, H. Lenske, K.-H. Behr, A. Brünle, K. Burkard, H. Irnich, T. Kobayashi, G. Kraus, A. Magel, G. Münzenberg, F. Nickel, K. Riisager, C. Scheidenberger, B.M. Sherrill, T. Suzuki, B. Voss, *Z. Phys.* A350 (1995) 283.
-
- [2] G. Audi, A.H. Wapstra, *Nucl. Phys. A* 565 (1993) 1.
- [3] P.G. Hansen, A.S. Jensen, B. Jonson, *Annu. Rev. Nucl. Part. Sci.* 45 (1995) 591.
- [4] Z. Ren, A. Faessler *J. Phys. G Nucl. Part.* (1998) 1823.
- [5] J.N. Bahcall, S. Basu, M.H. Pinsonneault, *Phys. Lett. B* 433 (1998) 1.
- [6] J.H. Kelley, Sam. M. Austin, A. Azhari, D. Bazin, J.A. Brown, H. Esbensen, M. Fauerbach, M. Hellström, S.E. Hirzbruch, R.A. Kryger, D.J. Morrissey, R. Pfaff, C.F. Powell, E. Ramakrishnan, B.M. Sherrill, M. Steiner, T. Suomijärvi, M. Thoennessen, *Phys. Rev. Lett.* 77 (1996) 5020.
- [7] F. Negoita, C. Borcea, F. Carstoiu, M. Lewitowicz, M.G. Saint-Laurent, R. Anne, D. Bazin, J.M. Corre, P. Roussel-Chomaz, V. Borrel, D. Guillemaud-Mueller, H. Keller, A.C. Mueller, F. Pougheon, O. Sorlin, S. Lukyanov, Yu. Penionzhkevich, A. Fomichev, N. Skobolev, O. Tarasov, Z. Dlouhy, A. Kordyasz, *Phys. Rev. C* 54 (1996) 1787.
- [8] A.S. Goldhaber, *Phys. Lett. B* 53 (1974) 306.
- [9] H. Esbensen, *Phys. Rev. C* 53 (1996) 2007.
- [10] H. Geissel, P. Armbruster, K.H. Behr, A. Brünle, K. Burkard, M. Chen, H. Folger, B. Franczak, H. Keller, O. Klepper, B. Langenbeck, F. Nickel, E. Pfeng, M. Pfützner, E. Roeckl, K. Rykaczewski, I. Schall, D. Schardt, C. Scheidenberger, K.-H. Schmidt, A. Schröter, T. Schwab, K. Sümmerer, M. Weber, G. Münzenberg, T. Brohm, H.-G. Clerc, M. Fauerbach, J.-J. Gaimard, A. Grewe, E. Hanelt, B. Knödler, M. Steiner, B. Voss, J. Weckenmann, C. Ziegler, A. Magel, H. Wollnik, J.P. Dufour, Y. Fujita, D.J. Viera, B. Sherrill, *Nucl. Instr. and Meth. B* 70 (1992) 286.
- [11] D. Cortina-Gil et al., to be published.
- [12] H. Geissel, GSI Report 97-03.
- [13] H. Lenske, *J. Phys. G: Nucl. Part.* 24 (1998) 1429.
- [14] T. Baker, L. Bimbot, C. Djalali, C. Glashauser, H. Lenske, W.G. Love, M. Morlet, E. Tomasi-Gustafsson, J. van der Wiele, J. Wambach A. Willis, *Phys. Rep.* 289 (1997) 235.

- [15] T. Baumann, H. Geissel, H. Lenske, K. Markenroth, W. Schwab, M.H. Smedberg, T. Aumann, L. Axelsson, U. Bergmann, D. Cortina-Gil, L. Fraile, M. Hellström, M. Ivanov, N. Iwasa, R. Janik, B. Jonson, G. Münzenberg, F. Nickel, T. Nilsson, A. Ozawa, A. Richter, K. Riisager, C. Scheidenberger, G. Schrieder, H. Simon, B. Sitar, P. Strmen, K. Sümmerer, T. Suzuki, M. Winkler, H. Wollnik, M.V. Zhukov, Phys. Lett B, (1998) *in press*
-
- [16] N. Iwasa, H. Geissel, G. Münzenberg, C. Scheidenberger, Th. Schwab, H. Wollnik, Nucl. Instrum. Meth. B 126 (1997) 284.
- [17] P.G. Hansen, Phys. Rev. Lett. 77 (1996) 1016.
- [18] K. Hencken, G. Bertsch and H. Esbensen, Phys. Rev. C 54 (1996) 3043.
- [19] D. Ridikas, M.H. Smedberg, J.S. Vaagen, M.V. Zhukov, Nucl. Phys. A 628 (1998) 363.
- [20] L.V. Grigorenko, B.V. Danilin, V.D. Efros, N.B. Shul'gina, M.V. Zhukov, Phys. Rev. C 57 (1998) R2099.
- [21] R. Serber, Phys Rev. 72 (1947) 1008.

Table 1

Summary of the widths for the longitudinal momentum distributions and the proton stripping cross sections. The numbers are calculated from equation (2) with the relative motion wave functions $F_{j_x j_y}(Y)$ obtained in Ref. [20]. The experimental width and one-proton removal cross-section obtained in this work are 91 ± 6 MeV/c and 98 ± 6 mb, respectively.

channel	$S_{j_x j_y}$	FWHM(Serb.)	FWHM(Absorp.)	σ_{-p}
(j_x, j_y)		(MeV/c)	(MeV/c)	(mb)
(3/2,3/2)	0.685	149	92	60
(3/2,1/2)	0.101	132	83	10
(1/2,3/2)	0.083	170	116	6.6
3 channels	0.869	149	92	77

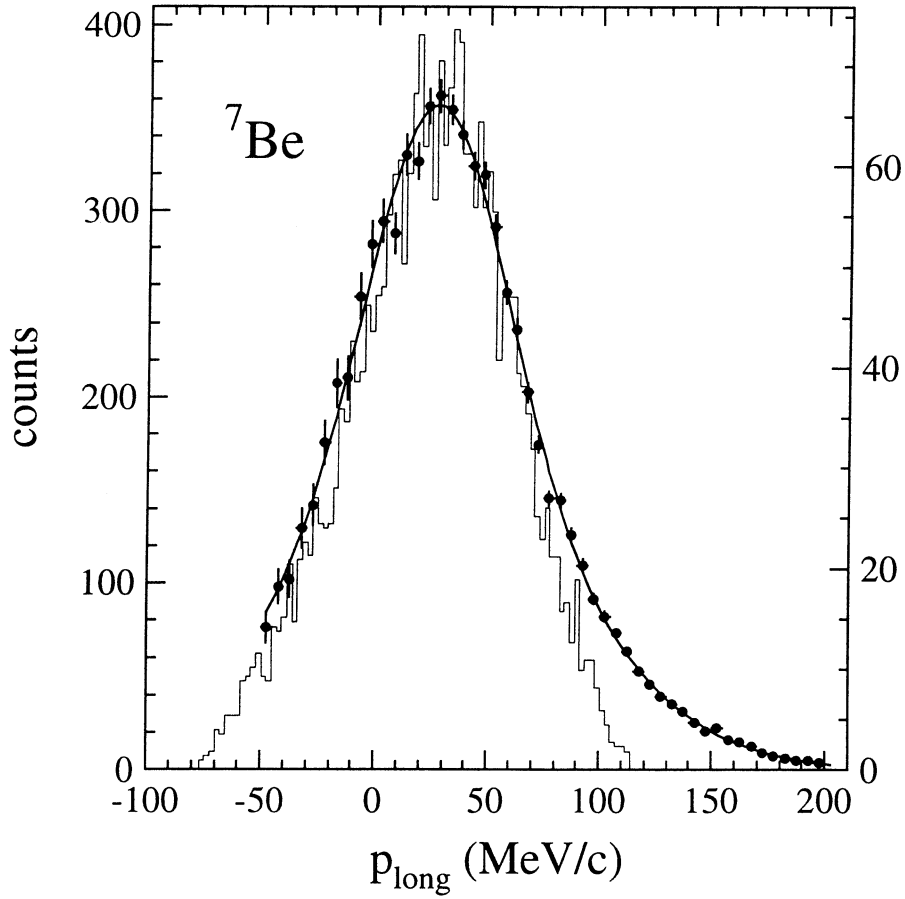


Fig. 1. The measured ${}^7\text{Be}$ momentum distribution from ${}^8\text{B}$ breakup reactions in a carbon target. The filled datapoints represent the data from this work while the histogram shows the distribution in the previous measurement [1].

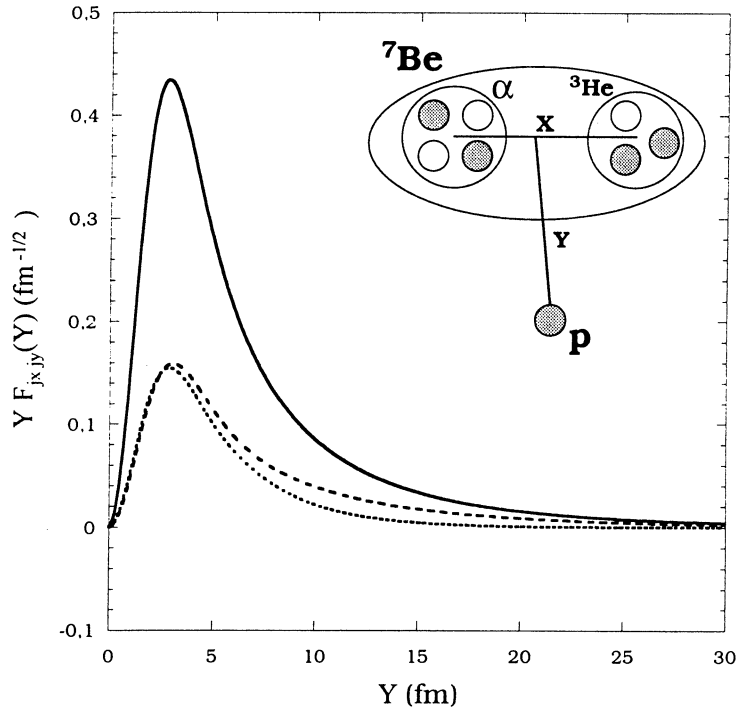


Fig. 2. Different ${}^7\text{Be}$ - p relative motion wave functions from [20] used in the calculations of the ${}^7\text{Be}$ momentum distribution for the proton-stripping channel of ${}^8\text{B}$ in a carbon target according to equation (1). The solid line corresponds to the ground state of ${}^7\text{Be}$ ($J^\pi = 3/2^-$) coupled to the valence $p_{3/2}$ proton, the dashed line to the ground state and the valence $p_{1/2}$ proton, and the dotted line to the first excited state of ${}^7\text{Be}$ ($J^\pi = 1/2^-$) coupled to the valence $p_{3/2}$ proton. The inset shows the definition of the (X,Y) coordinates in equation (1).

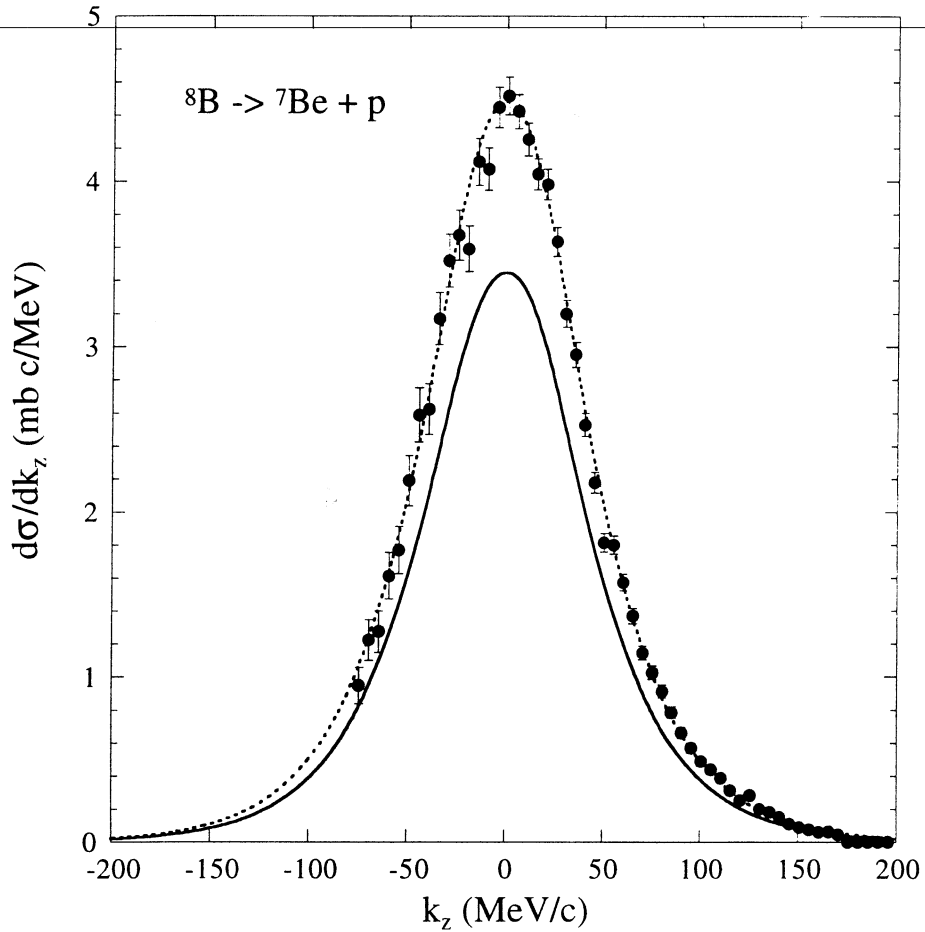


Fig. 3. Longitudinal momentum distribution of ${}^7\text{Be}$ fragments from ${}^8\text{B}$ breakup reactions. The experimental data are taken at 1440 MeV/u on a carbon target. The solid curve has been calculated for the ${}^8\text{B}$ wave function according to equation (2) with parameters $R_c=2.40$ fm, $R_t=2.47$ fm, and $R_p=0.8$ fm. The dotted curve is the same but normalized to the experimental data. The theoretical curves are convoluted with the experimental resolution that broadens the measured momentum distribution.